ELSEVIER

Contents lists available at ScienceDirect

## Computational Materials Science

journal homepage: www.elsevier.com/locate/commatsci



# A study of the hydrogen adsorption mechanism of $W_{18}O_{49}$ using first-principles calculations



Wenjie Liu, Pingguo Jiang\*, Yiyu Xiao, Jinsheng Liu

School of Metallurgical and Chemical Engineering, Jiangxi University of Technology and Science, Ganzhou, 341000, China

ARTICLE INFO

Keywords: First principles calculation  $W_{18}O_{49}$  $H_2$ Adsorption energy

#### ABSTRACT

Bulk and surface properties of  $W_{18}O_{49}$ , as well as the mechanism of hydrogen adsorption on  $W_{18}O_{49}$  (0 1 0) surface, were studied using first-principles calculation. The calculated results showed that the bulk  $W_{18}O_{49}$  has an indirect band gap of 0.75 eV, and the material exhibited certain metallicity. Moreover, the bulk  $W_{18}O_{49}$  is mainly composed of covalent bonding due to the strong resonance of WsbndO orbitals. The (0 1 0) surface of  $W_{18}O_{49}$  consists of the WO-terminated and O-terminated surface. Hydrogen adsorption on different sites of  $W_{18}O_{49}(0\,1\,0)$ , including  $P-O_{2c}$ ,  $V-O_{2c}$ ,  $P-O_{1c}$  and  $V-O_{1c}$ , was also investigated, and the result showed that the adsorption energy of  $P-O_{1c}$  and  $V-O_{1c}$  adsorption configurations are -6.13 and -6.807 eV, respectively, and thus possess the good stability. During the process of  $H_2$  adsorption on  $W_{18}O_{49}(0\,1\,0)$  surface. Hydrogen molecules are decomposed into two hydrogen atoms and adsorbed at the  $O_{1C}$  site. followed by the formation of water and oxygen vacancy on the  $W_{18}O_{49}$  surface.

#### 1. Introduction

 $W_{18}O_{49}$  is an n-type semiconductor and important functional material, which is extensively used in many fields, such as composite catalytic materials, gas-sensitive materials, photovoltaic materials, electro-photoluminescent/thermochromic materials and wave-absorbing materials [1–5]. Meanwhile, it is the main raw material for making ultra-fine tungsten powder. The tungsten, i.e. the reduced product of  $W_{18}O_{49}$ , is also widely applied in cemented carbide, tungsten based alloys, tungsten wire and tungsten electrodes due to its excellent physical and chemical properties, such as high melting point, high hardness and high elasticity modulus [7–9]. Currently, the preparation of tungsten products using traditional preparation technology can not meet the demand of markets. However, the tungsten products synthetizing from ultrafine tungsten powder could significantly improve their strength and toughness, and decrease plastic-brittle transition temperature [10–12].

Recently, the thermodynamics and kinetics of ultrafine tungsten powder preparation processes using hydrogen reduction have been extensively studied [6,13,14]. However, the adsorption kinetics in the microscopic scope of ultrafine tungsten powder preparation is still unclear. Actually, the first-principle method based on density functional theory (DFT) is a efficient tool to study the properties of structural and solid functional materials [15–16], as well as their reaction mechanisms

with gas-solid reaction [17-19].

In this paper, the first-principle calculation was conducted to investigate the bulk, surface properties of  $W_{18}O_{49}$ , and hydrogen adsorption behaviors on the  $W_{18}O_{49}$  (0 1 0). This aims to deeply understand the surface characteristics of  $W_{18}O_{49}$  and its reaction rules with  $H_2$  molecules, which could provide useful theoretical bases for ultrafine tungsten powder preparation.

#### 2. Calculation method and details

#### 2.1. Calculation method

All the calculations were performed within the framework of density functional theory using a basis set consisting of plane waves, as implemented in CASTEP (Cambridge Serial Total Energy Package)[20]. The electron-ion interactions were described by ultrasoft pseudopotentials, the Perdew-Burke-Ernzerhof (PBE) of the general gradient approximation (GGA) [21,22] was used to treat the electron exchange and correlation energies. The cutoff energy was set to 350 eV after convergence tests, the Brillouin zone was sampled with special k-points of a  $1 \times 5 \times 1$  grid for bulk  $W_{18}O_{49}$  and  $W_{18}O_{49}(0\ 1\ 0)[23]$ . Periodic boundary conditions were applied to all the models. The Broyden-Fletcher-Goldfarb-Shanno (BFGS)[24] algorithm was employed to optimize the molecular geometries. The calculation accuracy was set as

E-mail address: pingguo\_jiang@163.com (P. Jiang).

<sup>\*</sup> Corresponding author.

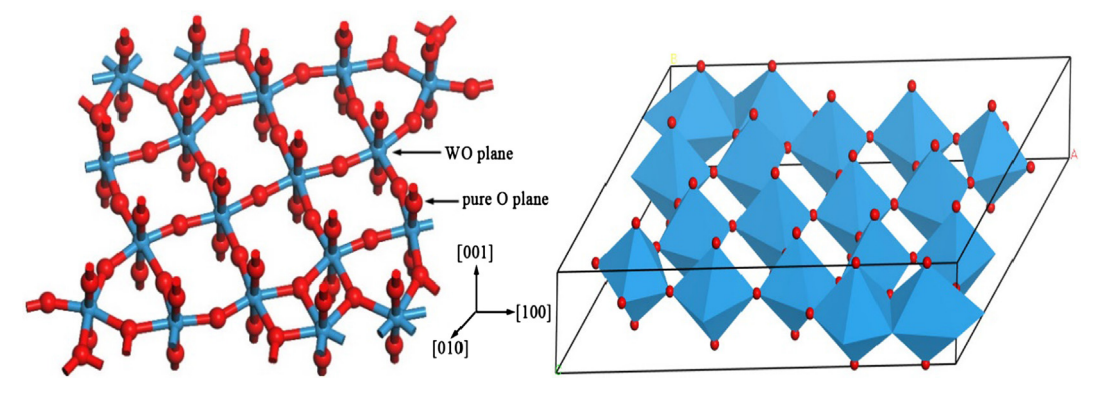


Fig. 1. Schematic diagram of  $W_{18}O_{49}$  crystal structure. Red and blue balls denote O and W atoms, respectively. (For interpretation of the references to colour in this figure legend, the reader is referred to the web version of this article.)

fine grade with the energy tolerance of  $1.5 \times 10^{-5}\,\text{eV/atom}$ , force tolerance of  $0.3\,\text{eV/nm}$ , and displacement tolerance of  $1.0 \times 10^{-4}\,\text{nm}$ . The Fermi smearing was  $0.1\,\text{eV}$ . The atomic orbital of W, O and H were set as  $5s^25p^65d^46s^2$ ,  $2s^22p^4$  and 1s, respectively. All calculations were carried out at 0 K. Convergence tests were performed carefully to make sure the atom layers and vacuum are enough thick for our calculations. The atoms in all layers were allowed to relax during the surface structure optimization.

#### 2.2. Calculation models

The bulk  $W_{18}O_{49}$  is a monoclinic crystal with a non-stoichiometry and asymmetric structure, as shown in Fig. 1. It belongs to the P2/m space group with octahedron structure [25], and the coordination numbers of W and O are 6 and 2, respectively.

#### 2.3. $W_{18}O_{49}$ (0 1 0) structure model

The  $W_{18}O_{49}\ (0\ 1\ 0)$  surface with the lowest surface energy has two different terminations [25], i.e. WO-terminated and O-terminated  $W_{18}O_{49}\ (0\ 1\ 0)$ , as shown in Fig. 2. The  $W_{5c}$  and  $W_{6c}$  in Fig. 2 are 5-coordinated and 6-coordinated W atoms, while the  $O_{1c}$  and  $O_{2c}$  are 1-coordinated and 2-coordinated O atoms. Each surface model contains 5 layers, and a vacuum of 1.0 nm was added on the slab structure. The thickness of vacuum and atomic layers were determined after the convergence test.

It is well known that the reaction between  $W_{18}O_{49}$  and  $H_2$  leads to the formation of W and  $H_2O$  [26]. Therefore,  $H_2$  molecular adsorption on four different positions of  $W_{18}O_{49}$  (0 1 0) surface were constructed. As shown in Fig. 3, in the V-O<sub>2c</sub> (P-O<sub>2c</sub>) configuration, the hydrogen molecules were preset vertical (parallel) to WO-terminated (0 1 0) surface (Fig. 3a and b); in the V-O<sub>1c</sub> (P-O<sub>1c</sub>) configuration, the hydrogen

molecules were preset vertical (parallel) to O-terminated (0  $1\,0$ ) surface (Fig. 3b and d).

#### 3. Results and discussion

#### 3.1. Bulk properties

The calculated lattice constants of bulk  $W_{18}O_{49}$ :  $a=1.8536\,\text{nm},$   $b=0.3815\,\text{nm},$   $c=1.4211\,\text{nm},$   $\beta=115.3^\circ,$  which agrees well with the experimental datas [25–26]. The calculated band structure and partial density of state (PDOS) of bulk  $W_{18}O_{49}$  are presented in Figs. 4 and 5, respectively. It can be seen from Fig. 4 that the conduction band minimum (CBM), valence band maximum (VBM) and band gap (indirect type) are  $-0.93\,\text{eV},$   $-1.68\,\text{eV}$  and  $0.75\,\text{eV}$ , respectively. The Fermi level passing through the energy band indicates the  $W_{18}O_{49}$  crystal has certain metallic characteristics. However, the experimental result suggests the bulk  $W_{18}O_{49}$  possesses semiconducting properties due to its surface covered with oxygen atoms. In WOx, the larger the x is, the smaller the charge carrier concentration is, and the Fermi level shifts to the band gap, which results in the change from metallic to semiconductive for  $W_{18}O_{49}$ .

The total density of state (TDOS) and partial density of state (PDOS) of bulk  $W_{18}O_{49}$  are shown in Fig. 5. The conduction band of  $W_{18}O_{49}$  is dominated by O-2p and W-5d states. The obvious orbital hybridizations between the W-d and O-p states in the ranges of -9.1 to -1.7 eV and -18.5 to -16.5 eV are found, which indicates the strong covalent bonding is formed. In addition, the weak interaction between W-p and O-p orbitals from -40 to -38 eV is also observed. Moreover, the pseudogap near the Fermi level indicates the existence of the covalent bonding. Also, a flat band appears at -0.93 eV near the bottom of the conduction band. The existence of flat band is ascribed to the defect formation for unpaired W-5d electrons or unpaired W atoms.

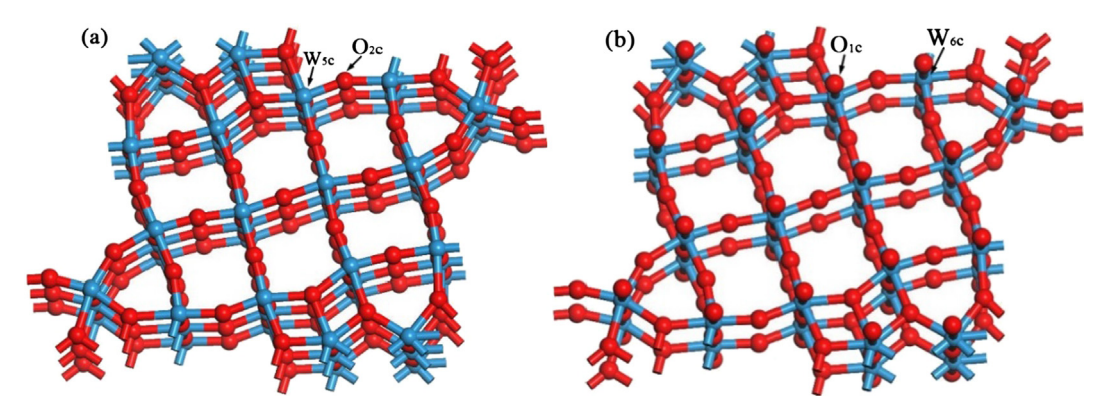


Fig. 2.  $W_{18}O_{49}$  (0 1 0) surface structures: (a) WO-terminated (0 1 0) surface; (b) O-terminated (0 1 0) surface. Red and blue balls denote O and W atoms, respectively. (For interpretation of the references to colour in this figure legend, the reader is referred to the web version of this article.)

### Download English Version:

# https://daneshyari.com/en/article/10155822

Download Persian Version:

https://daneshyari.com/article/10155822

<u>Daneshyari.com</u>